

**SYNTHESIS, CHARACTERIZATION, DNA DEGRADATION,
FREE RADICAL SCAVENGER AND ANTIBACTERIAL
ACTIVITIES OF BINUCLEAR CO(II), CU(II) AND
MONONUCLEAR NI (II) COMPLEXES OF NOVEL
BULKY MULTI-DENTATE THIOSEMICARBAZIDE**

O. A. El-Gammal*, A.A.El-Asmy and I.M.Abd Al-Gader
Department of Chemistry, Faculty of Science, Mansoura University,
Mansoura, 35566, P.O.Box 70, Mansoura- Egypt.

(Received: 13/ 4/ 2013)

ABSTRACT

The chelation behavior of multi-dentate thiosemicarbazide, 2,2'-((9S,10S,11R,12R)9,10-dihydro-9,10-ethanoanthracene-11,12-dicarbonyl)bis(N-ethylhydrazine-1-carbothioamide)(H₆ETS)(1) towards Co²⁺, Ni²⁺ and Cu²⁺ ions have been studied. The structures of the complexes were elucidated by conventional measurements. The data revealed that the ligand acts as mononegative either as NNS tetradentate in Cu (II) complex (2) or ONS hexadentate donor in Co(II)(3) and Ni(II)(4) complexes. According to electronic spectra and magnetic moment measurements, a square planar geometry for Ni(II) and Cu(II) complexes and a tetrahedral arrangement for Co(II) complex were proposed. The EPR spectrum of Cu²⁺ complex simulated with an axial spin-Hamiltonian exhibits a four-line pattern with nitrogen super-hyperfine couplings originating from. The planar complex possess a significant amount of tetrahedral distortion leading to a pseudo-square planar geometry with unpaired electron has d_{x²-y²} ground state. The bond length and bond angle have been calculated. Also, the thermal behavior and kinetic parameters were determined using Coats-Redfern and Horowitz-Metzger methods. Furthermore, the title compounds were investigated for their antibacterial activity against *Staphylococcus epidermalis* (*St.epid*); *Streptococcus pyogenes* (*Strp.py.*) as Gram +ve bacteria and *Escherichia Coli* (*E.coli*); *klebsiella Spp* (*kleb.spp.*) as Gram - Ve bacteria using inhibition zone diameter. Also, the compounds were tested for DNA degradation, superoxide-scavenging activity in the PMS/NADH-NBT system as well as their scavenging effect on hydroxyl radicals that generated by the oxidation of cytochrome c in l-ascorbic acid/CuSO₄-cytochrome c system. imine hydrazinic nitrogen atoms.

Keywords: multi-dentate thiosemicarbazide, thermal, modeling, antibacterial, hydroxyl radical and superoxide dismutase.

1. INTRODUCTION

Over the last decades, thiosemicarbazide compounds are very promising in coordination chemistry due to their chemistry and potentially beneficial biological activities such as antitumor (Ali et al., 2001 ; Ferrari et al., 1999 and Campbell 1975) antibacterial (Petering & Burskirk, 1967; Mcmillian et al., 1986; Bouwman, & Driessen, 1990 and West et al., 1991), antiviral and antimalarial activities (West et al., 1993; Wada et al., 1994 and Alsop et al., 2005). The biological activity of thiosemicarbazides is related to their versatile nature coordinating to the metal ion either as a neutral ligand or as a deprotonated ligand through S, N, N atoms (Mostafa 2007) or O, N and S atoms (Alliage and Lissi., 1998; Lissi et al., 1999; El-Gazzar et al., 2009) or sometimes through O, N, N atoms (Aeschlach et al., 1994). The presence of bulky substituent at the N(4) in the thiosemicarbazide chain led to an enhancement of antimicrobial activity relative to the unsubstituted analogs, probably due to an increase in lipophilicity (Delley 1990; Delley 1998; Delley 2000; Delley 2002; Kessi & Delley, 1998 and Materials studio, 2009) which is related to the tendency of a molecule to be transported through biological membranes. The metal in the complex has its own influence in increasing the overall activity of the complex compared to the free ligand through a synergic effect. The ligands containing N, O and S atoms play a major role in their binding to DNA. Also, large planar thiosemicarbazides were found to promote intercalative binding of metal complexes to DNA, whereas the central metal ion plays a crucial role in the cleavage of DNA. On continuation of our work (Mostafa 2007), we describe herein the synthesis, spectral and thermal studies of new series of binuclear Co(II), Cu(II) and mononuclear Ni(II) complexes derived from 2,2'-((9S,10S,11R,12R)9,10-dihydro-9,10-ethanoanthracene-11,12-dicarbonyl) bis (N-ethylhydrazine-1-carbothioamide) (H₆ETS). The degradation kinetics have been studied by Coats-Redfern and Horowitz-Metzger methods. Thermodynamic parameters (ΔS , ΔH and ΔG), have been evaluated using the standard equations. Finally, the scavenging effects of all compounds on free radical are evaluated. Recently,

antioxidants that exhibit SOD and hydroxyl radical scavenging activities are increasingly receiving attention. Literature survey shows no studies of the radical scavenging of the thiosemicarbazide under investigation has yet been undertaken. Accordingly, a study of new thiosemicarbazide derivative with antioxidant activity would support the development of new drugs and improve the treatment of various diseases.

2. EXPERIMENTAL

2.1. Instrumentation and materials

All the chemicals were purchased from Aldrich and Fluka and used without further purification. Elemental analyses (C, H, N) were performed with a Perkin-Elmer 2400 series II analyzer. Molar conductance values (10^{-3}molL^{-1}) of the complexes in DMF were measured using a Tacussel conductivity bridge model CD6NG. IR spectra ($4000\text{-}400\text{ cm}^{-1}$) in KBr discs were recorded on a Mattson 5000 FTIR spectrometer. Electronic spectra were recorded on a Unicam UV-Vis spectrophotometer UV2. Magnetic susceptibilities were measured with a Sherwood scientific magnetic susceptibility balance at 298 K. $^1\text{H-NMR}$ measurements in $d_6\text{-DMSO}$ were carried out on a Varian Gemini WM-200 MHz spectrometer. Mass spectrum was recorded on a Varian Mat 311. Thermal measurements (TGA, DTA, $20\text{-}1000^\circ\text{C}$) were recorded on a DTG-50 Shimadzu thermo-gravimetric analyzer at a heating rate of $15^\circ\text{C}/\text{min}$ and nitrogen flow rate of $20\text{ ml}/\text{min}$. ESR spectra were obtained on a Bruker EMX spectrometer working in the X-band (9.78 GHz) with 100 kHz modulation frequency. The microwave power and modulation amplitudes were set at 1 mW and 4 Gauss , respectively. The low field signal was obtained after 4 scans with 10 fold increase in the receiver again. A powder spectrum was obtained in a 2 mm quartz capillary at room temperature.

2.2. Synthesis of H_6ETS

H_6ETS was synthesized by heating 9,10-dihydro-9,10-ethanoanthracene-11,12-diacidhydrazide (Hehre et al., 1986) with ethylisothiocyanate in a 2:1 molar ratio under reflux for 4 h. The white precipitate that formed was filtered off, washed several times with ethanol and dried in a desiccator under vacuum over anhydrous CaCl_2 . It was checked by TLC, partial elemental analysis (C, H and N), spectral (IR, UV-Vis., $^1\text{H NMR}$) and mass spectra.

2.3. Synthesis of complexes

Ethanol solution of H₆ETS (0.496 g, 1.0 mmol) and hydrated metal chloride salts (Co, Ni and Cu (2.0 mmol) were heated under reflux for 5 h. The precipitates formed were filtered off, washed with hot ethanol followed by diethyl ether and dried in a vacuum desiccator over anhydrous CaCl₂.

2.4. Biological applications

2.4.1. Antibacterial activity

The antibacterial investigation of H₆ETS and its metal complexes was carried out using cup diffusion technique, developed by Kirby-Bauer. The test was done against the *Staphylococcus epidermalis* (Hammer et al., 1999) (St.epid); *Streptococcus pyogenes* (Strp.py.) as Gram +ve bacteria and *Escherichia Coli* (E.coli) ; *klebsiella* Spp (kleb.spp.) as Gram -Ve bacteria organisms. The tested free ligand and its complexes were dissolved in DMSO at concentration 1 mg/mL. The Luria-Bertani Agar (LBA) medium was used. An aliquot of the solution of the tested complexes equivalent to 100 µg was placed separately in each cup. The LBA plates were incubated for 24 h at 30-37°C for overnight. DMSO was used as a -ve control for this test and the Ampicilline was utilized as a +ve control. Each inhibition zone was measured three times by caliper to get an average value. The test was performed three times for each bacterium culture. The larger the clear area around the filter disk, the more effective the compound

2.4.2. DNA cleavage studies

A solution of 2 mg of Calf thymus DNA was dissolved in 1 ml of sterile distilled water. Stock concentrations of the investigated ligand and its complexes were prepared by dissolving 2 mg/ml DMSO. Equal volumes from each compound and DNA were mixed thoroughly and kept at room temperature for 2-3 h. The effect of the chemicals on the DNA was analyzed by agarose gel electrophoresis. A 2 µl of loading dye were added to 15 µl of the DNA mixture before being loaded into the well of an agarose gel. The loaded mixtures were fractionated by electrophoresis, visualized by UV and photographed (Matveev et al., 1999).

2.4.3. Superoxide dismutase (SOD) scavenging activity

Scavenging activity of superoxide radicals was determined as described (Geary, 1971). SOD activity of the investigated compounds was assayed by using phenazene methosulfate (PMS) to photogenerate a reproducible and constant flux of superoxide anion radicals at pH=8.3 (phosphate buffer). Reduction of nitroblue tetrazolium(NBT) to blue formazan was used as an indicator of O_2^- production and followed spectrophotometrically at 560 nm. The addition of PMS ($9.3 \times 10^{-4}M$) to an aqueous solution of NBT ($3.0 \times 10^{-5} M$), NADH (nicotine amide adinine dinucleotide, $4.7 \times 10^{-4}M$) and phosphate buffer (final volume of 2 ml) caused a $\Delta OD(\Delta 560)/\text{min}$ change. The reaction in blank samples and in presence of the compounds under study was measured for 5 minutes. The inhibition percent was calculated using the equation:

$$\% \text{ Inhibition} = \Delta B - \Delta S / \Delta B \times 100$$

Where $\Delta B = A_{5\text{min}} - A_{\text{zero}}/5$; is the change in absorbance from 0 to 5 minutes for the standard i.e. ascorbic acid(B) and the sample (S), respectively.

2.4.4. Scavenging activities of hydroxyl radicals

Scavenging activity of hydroxyl radicals was determined (West et al., 1999). The hydroxyl radicals were generated in the l-ascorbic acid- $CuSO_4$ system by reduction of Cu^{2+} and were assayed by the oxidation of cytochrome c. The hydroxyl radicals were generated in 2 ml of 10 mM sodium phosphate buffer (pH 7.4), containing 100 μM l-ascorbic acid, 100 μM $CuSO_4$, 12 μM cytochrome c and H_2O_2 and its metal complexes (10 μM). The change in absorbance caused by the oxidation of cytochrome c was measured at 550 nm. Thiourea was used as a positive control. The scavenging activity of hydroxyl radical was calculated using the following formula:

$$\text{Hydroxyl radical scavenging activity (\%)} = (A - A_0 / A_T - A_0) \times 100$$

where A is the absorbance of samples, and A_T and A_0 are the absorbance of the thiourea and the control, respectively.

2.5. Molecular modeling

An attempt to gain a better insight on the molecular structure of the ligand and its complexes, geometry optimization and conformational analysis has been performed by the use of MM+ force-field (Rao & Venkataraghavan, 1962) as implemented in hyperchem 8.0 (Li et al., 2003). The low lying obtained from MM+ was then optimized at PM3

using the Polak-Ribiere algorithm in RHF-SCF, set to terminate at an RMS gradient of $0.01 \text{ kcal mol}^{-1}$.

3. RESULTS AND DISCUSSION

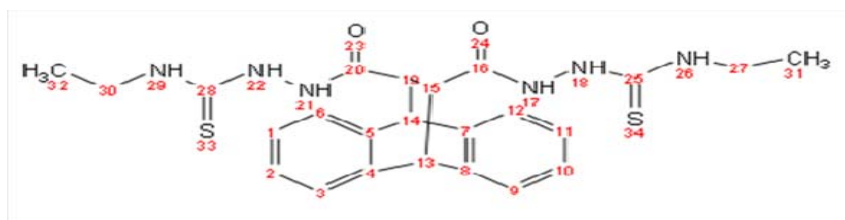
The formulae of the complexes, physical properties, elemental analysis and formula weights obtained for some complexes from mass spectra are listed in **Table 1**. The isolated complexes, are quite stable in air, non-hygroscopic and insoluble in water and most organic solvents but soluble in DMF and DMSO. The molar conductivity in DMF solution at 25°C for all complexes in general are in the $11\text{-}20 \text{ ohm}^{-1} \text{ cm}^2 \text{ mol}^{-1}$ range indicating non-electrolytic nature (**Braibanti et al., 1968**).

Table(1): Physical properties and elemental analyses of H_6ETS and its complexes.

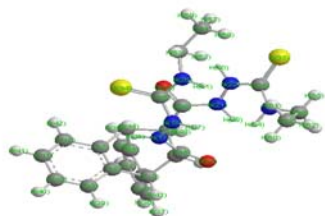
Compound, Formula	F.Wt	Colour	Yield %	M.P., $^\circ\text{C}$	Found (Calcd.) %				
					C	H	N	Cl	M
H_6ETS	496.65	White	90	260	58.62 (58.04)	5.49 (5.68)	15.89 (16.92)	----	---
$[\text{Co}_2(\text{H}_4\text{ETS})\text{Cl}_2] \cdot 10 \text{H}_2\text{O}$	863.56	Pale Green	88	>300	33.17 (33.38)	5.43 (5.37)	9.25 (9.73)	8.01 (8.21)	13.01 (13.65)
$[\text{Ni}(\text{H}_5\text{ETS})(\text{OH})]\text{H}_2\text{O}$	589.36	Biege	75	274	48.44 (48.91)	5.92 (5.13)	14.32 (14.26)	---	10.08 (9.96)
$[\text{Cu}_2(\text{H}_4\text{ETS})\text{Cl}_2] \cdot 2\text{H}_2\text{O}$	728.66	Pale Green	80	>300	40.52 (39.56)	5.49 (4.15)	11.23 (11.53)	9.57 (9.73)	17.93 (17.44)

3.1. Molecular modeling

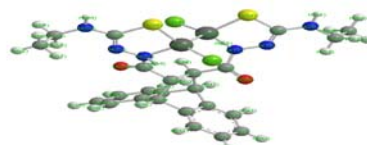
The molecular structure along with atom numbering of H_6ETS and its metal complexes are shown in structures (1-4). The obtained data are calculated using quantum mechanics for the complexes. A glance at data in **Tables S1-S8** indicates the following remarks:



(a)

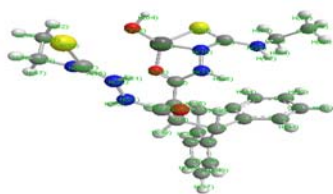


structures 1

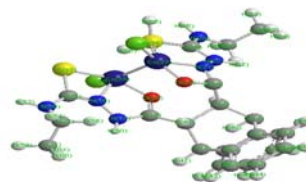


structures 2

(b)



structures 3



structures 4

1. The N(17)-N(18), N(21)-N(22), C(16)-N(17), C(20)-N(21), C(25)-S(34) and C(28)-S(33), bond lengths in H₆ETS become slightly longer in complexes as the coordination takes place via N atoms of -C=N- group that is formed on deprotonation of OH group or SH group in all complexes (**Bullo & Tajmir-Riahi, 1978**).

2. The C(16)-O(24) and/ or C(20)-O(23), C(25)-S(34) and / or C(28)-S(33) bond distances in all complexes become longer due to the formation of the M-O and M-S bonds which make the C-O and C-S bonds weaker (**Rapheal, et al., 2007**).

3. C(16)-N(17) and C(20)-N(21) bond distances in [Cu₂(H₄ETS)(Cl)₂].2H₂O and [Co₂(H₄ETS)(Cl)₂].10H₂O complexes and C(16)-N(17) bond distance in [Ni(H₃ETS) (OH)] .H₂O complex are elongated. This is referred to the formation of the M-O bond which makes the C-O bond weaker and forming a double bond character (**Nomiya, et al., 2004**).

4. The bond angles of the hydrazine moiety of H₆ETS are altered somewhat upon coordination; the largest change affects C(2)-N(3)-N(6) and O(4)-C(2)-N(3) angles which are reduced or increased on complex formation as a consequence of bonding (**Nomiya, et al., 2004**).

5. The C(16)-N(17)-N(18) and C(20)-N(21)-N(22) angle changes from 120.7°, 121.5° in the ligand to 122.8° or 117.6° in [Cu₂(H₄ETS)(Cl)₂].2H₂O and [Co₂(H₄ETS)(Cl)₂].10H₂O complexes due to the formation of the N(17)-Cu(34)-S(37), N(21)-Cu(33)-S(38), and N(18)-Co(34)-S(37), N(21)-Co(33)-S(38), chelate ring (**Bullok & Tajmir-Riahi, 1978**). The bond angles, N(18)-Co(34)-S(37), N(21)-Co(33)-S(38), N(18)-Co(34)-Cl(35), N(21)-Co(33)-Cl(36) and N(18)-Co(34)-O(24), N(21)-Co(33)-O(23) of 72.4°, 122.6°, 108.4°, 118.6°, 85.7° and 71.6° in [Co₂(H₄ETS)(Cl)₂].10H₂O complex indicate that the complex adopts a tetrahedral arrangement. On the other hand the bond angles in [Cu₂(H₄ETS)(Cl)₂].2H₂O and [Ni(H₅ETS)(OH)].H₂O complexes are quite near to a square planar geometry predicting sp³ and dsp³ hybridization. The complexes can be arranged according to M-N_{azomethine} and M-O bond lengths as follows: (M-N): Cu(33)-N(21), Cu(34)-N(17) > Co(34)-N(18), Co(33)-N(21) > Ni(32)-N(18); (M-S): Cu(33)-S(38), Cu(34)-S(37) > Co(33)-S(38), Co(34)-S(37) > Ni(32)-S(34); (M-O): Co(33)-O(23) > Ni(32)-O(23), reflecting the great strength of the Cu-N and Co-O bonds.

6. The lower HOMO energy values show that molecules donating electron ability is the weaker. On contrary, the higher HOMO energy implies that the molecule is a good electron donor. LUMO energy presents the ability of a molecule receiving electron (**El-Shazly, et al., 2004**).

7. The bond angles within the hydrazone backbone do not change significantly but the angles around the metal undergo appreciable variations upon changing the metal center (**Nakamoto, 1970**).

3.2. IR Spectra

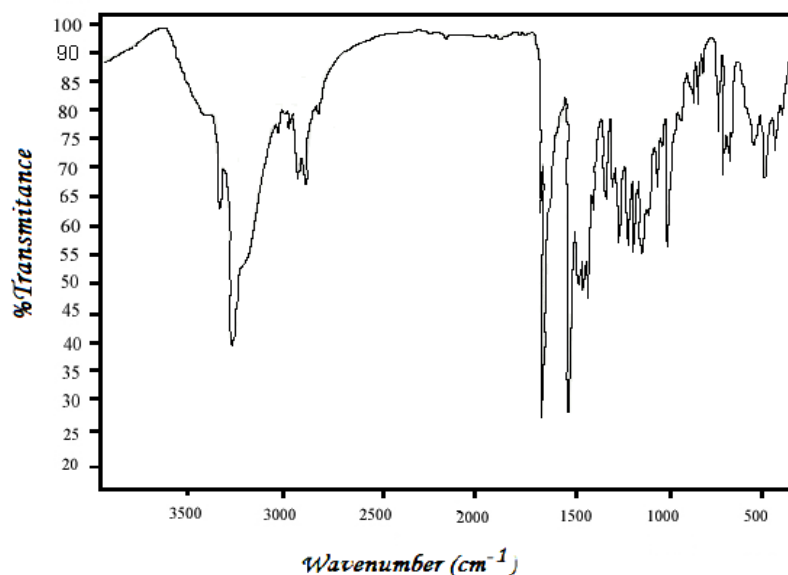
The most important IR bands of H₆ETS (Structure 1) and its complexes with probable assignments are given in (**Table 2**). A comparison of the spectra of H₆ETS and its complexes reveals that the ligand coordinates in thione -enol and thiol-keto forms. As the thiosemicarbazide molecule (**Structure 1**) is asymmetric, the two sharp bands at 1711 and 1684 cm⁻¹ in its IR spectrum of the ligand are

attributable to the stretching vibration modes of the two $(\text{C}=\text{O})^1$ and $(\text{C}=\text{O})^2$ groups (Aggrawal, & Narang, 1973) which oriented themselves in opposite direction to each other as confirmed by molecular modeling (Rao & Venkataraghavan, 1962). In complexes, the band due to $(\text{C}=\text{O})^1$ disappears suggesting enolization followed by deprotonation while the second band undergoes red shift as a result of coordination to the metal ion. The bands at 3371, 3289 and 3218 cm^{-1} are assignable to $\nu(\text{N}^4\text{H})$, $\nu(\text{N}^1\text{H})$ and $\nu(\text{N}^2\text{H})$ modes, respectively (Jones, 1958). The broadness of the bands due to $\nu(\text{N}^2\text{H})$ and $\nu(\text{N}^1\text{H})$ may be due to the chance of H-bond formation as in Structure I. The stretching and bending vibrations (ν/δ) of C=S groups are observed as strong bands at 1300 and 798 cm^{-1} , respectively (Chikate, et al., 2005 and Abou-Melha & Farukj, 2008). In all complexes these two bands are found to undergo weakness confirming the coordination via the thiolate or thione sulfur atom (El-Gammal & El-Asmy, 2008). The bands located at 1469, 1270 and 920 cm^{-1} assigned to thioamide I-V vibrations have substantial contributions from $\delta(\text{C}-\text{H})$, $\delta(\text{N}-\text{H})$ and $\nu(\text{C}=\text{S})$ vibrations (Lever, 1984). In the spectra of all complexes, the bands assigned to the newly formed $(\text{N}=\text{C})^*$ group due to the enolization or thioenolization of the H₆ETS are located in the range 1551-1615 cm^{-1} . Also, the strong band observed at 1135 cm^{-1} is assignable to the $\nu(\text{N}-\text{N})$ vibrational mode (El-Metwally et al., 2005). The doublets at 2931 and 2971 cm^{-1} are attributed to symmetric and asymmetric stretching vibrations of S-CH₂-CH₃ and CH groups. Also, the band at 3060 cm^{-1} is due to aromatic CH vibration. The possibility of thione/thiol tautomerism in the solid state is ruled out, since no characteristic for thiol group (2500-2650 cm^{-1}) is observed in the spectrum of the ligand (Lever, 1968).

Table (2): I.R. absorption spectral bands of H₆ETS and its metal complexes.

Compound	$\nu(\text{N}^4\text{H})$	$\nu(\text{N}^2\text{H})$	$\nu(\text{N}^1\text{H})$	$\nu(\text{C}=\text{O})$	$\nu(\text{C}=\text{S})$	$\nu(\text{C}=\text{C})$	$\nu(\text{C}=\text{N})$	$\nu(\text{C}-\text{S})$
H ₆ ETS	3371 _s	3289 _s	3218 _w	1711 _m 1684 _s	1300 _s 797 _s 744 _s	1597 _m	-	-
[Cu ₂ (H ₄ ETS)Cl ₂].2H ₂ O	3387 _w	-	3140 _b	1736 _m 1682 _s	-	1597 _m	1551 _m	629 _s
[Co ₂ (H ₄ ETS)Cl ₂].10H ₂ O	3363 _w	3283 _w	-	- 1666	1300 _w 797 _w	1593 _m	1563 _m	657 _s
[Ni(H ₅ ETS)(OH)].H ₂ O	3371 _m	3280 _w	3218 _m	1712 _m 1683	1300 _w 798 _s 745 _s	1595 _m	1615 _m	618 _s

S= strong, m= medium, b= broad and w = weak

**Fig. (1)**

Based on the above IR spectral evidences, it is confirmed that in copper complex (Structure 2) H₆ETS acts as mononegative NSSN tetradentate via the nitrogen atoms of two N¹H groups from both sides and both thiolate sulfur atoms as supported by disappearance of bands due to $\nu(\text{N}^2\text{H})$ and $\nu(\text{C}=\text{S})$ modes with simultaneous appearance of new bands at 1551 and 629 cm⁻¹ assignable to $\nu(\text{N}=\text{C})^*$ and $\nu(\text{C}-\text{S})$ modes,

respectively. The bands due to both C=O groups remain at the same positions confirming that they are not involved in coordination.

Molecular Structure of $[\text{Cu}_2(\text{H}_4\text{ETS})(\text{Cl})_2] \cdot 2\text{H}_2\text{O}$ complex In nickel complex (Structure 3), H_6ETS behaves as mononegative NSO tridentate through the nitrogen atom of $(\text{N}=\text{C})^*$, $(\text{C}=\text{O})^1$ and $(\text{C}-\text{S})$ centers. This is confirmed by i) the slight weakness of the bands at 1711 and 1683 cm^{-1} suggesting the bonding through one of the carbonyl groups, ii) the bands due to δ/ν ($\text{C}=\text{S}$) and (N^2H) modes undergo weakness as a result of coordination and iii) the appearance of new bands at 1615 and 618 cm^{-1} assignable to $\nu(\text{N}=\text{C})^*$ and ν ($\text{C}-\text{S}$) and (N^2H) modes.

The IR spectrum of cobalt complex (Structure 4) shows that, the ligand coordinates as binegative $\text{N}_2\text{S}_2\text{O}_2$ hexadentate through the two new $(\text{N}=\text{C})^*$, $\text{C}=\text{O}$, $\text{C}-\text{O}$, $\text{C}=\text{S}$ and $\text{C}-\text{S}$ groups. This behavior is revealed by the shift of the band at 1684 cm^{-1} in the spectrum of the ligand to 1666 cm^{-1} and weakness of the bands due to δ/ν ($\text{C}=\text{S}$) and (N^2H) modes. The increase of $\nu(\text{N}-\text{N})$ from 1135 to 1162 and 1160 cm^{-1} in the IR spectra of the complexes is due to the increase in the double bond character of $\text{N}-\text{N}$ offsetting the loss of electron density via donation to the metal ion and is a further evidence of coordination of the ligand through the azomethine nitrogen atom [28]. The appearance of new bands at 491,500 and 451,450 cm^{-1} assignable to $\nu(\text{M}-\text{O})$ and $\nu(\text{M}-\text{N})$ vibrations supports the mode of chelation [26]. Finally, the broad bands at $\approx 3399-3454$, 868-850, and at $\approx 567\text{cm}^{-1}$ in the IR spectra of the investigated complexes are referred to stretching, $\nu(\text{OH})$, rocking, δ_r (H_2O), and wagging, δ_w (H_2O), vibration motions of coordinated water molecules confirming the existence of water molecules inside the coordination sphere. Also, the broad band centered at 3500 cm^{-1} in the spectra of the studied complexes may be due to hydrated water. This notification will be supported by thermal analysis.

3.3. $^1\text{H-NMR}$

The ^1H NMR spectrum of the H_6ETS in $d_6\text{-DMSO}$ (Fig.1) reveals signals at 10.00, 9.82 and 7.57 ppm are assigned to N^1H , N^2H and N^4H protons, respectively. These protons appear as singlet as expected since the NH protons are decoupled from the nitrogen atoms and the protons from the adjacent atoms and disappear on addition of D_2O . The signals due to CH_2 protons appeared as a two quartets one at 4.78 ppm (q, $J=7.5$, 2H) and the other at 2.49 ppm. The signals due to CH_3 protons appear as a triplet at 1.02 ppm (t, $J=7.0$, 3H) and singlet at 1.24 ppm.

Moreover, the protons of CH groups (CH13-CH14) appear at 3.34, 3.22 (dd, $J=3.6$, 1H) and (CH15-CH19) as multiplet at 3.42-3.50 ppm. According to the above, it may be suggested that the thiosemicarbzide can exist in more than one conform arising with different orientations with respect to the $\text{CH}_3\text{-CH}_2$ group. Also, the absence of a signal due to SH or OH suggesting the presence of ligand in the thione-keto form in the solution as shown in structure I (El-Asmy *et al.*, 1990).

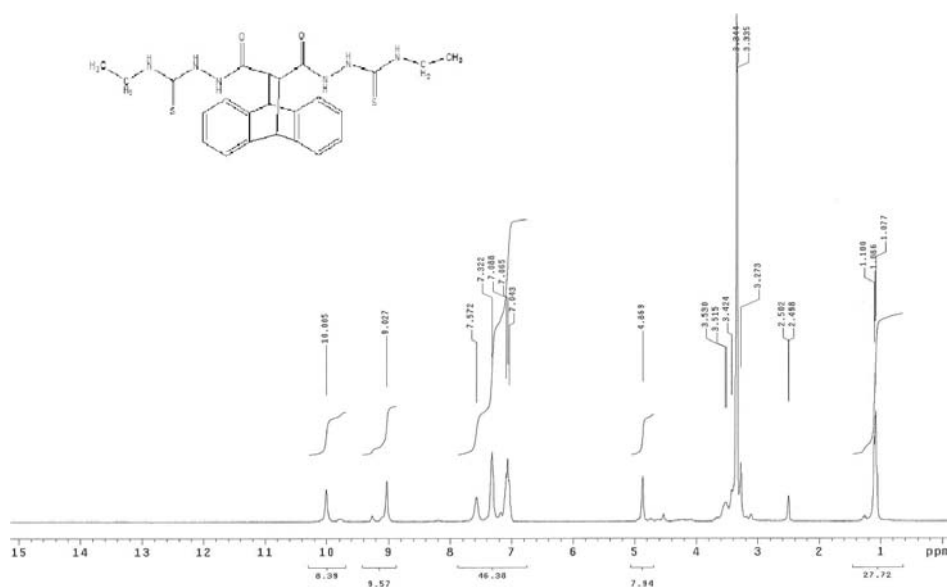


Fig.(2)a. The ¹H MNR spectrum of H₆ETS in d₆-DMSO

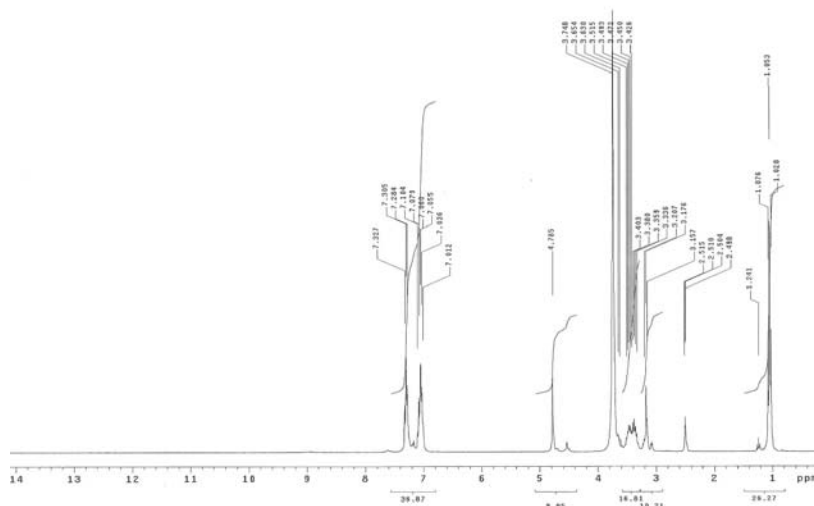


Fig. (2)b. The ^1H MNR spectrum of H_6ETS in D_2O .

3.4. Electronic spectra and magnetic moments

The magnetic moments and the significant electronic absorption bands of H_6ETS and its complexes, in DMSO and Nujol mull, are given in Table 3. The electronic spectra of the complexes are dominated by intense intra-ligand charge-transfer bands. The ligand shows two broad bands at 36496 and 26453 cm^{-1} , presumably arising from $(\pi \rightarrow \pi^*)$ and $n \rightarrow \pi^*$ {a combination of the transitions due to those of benzene ring, carbonyl and thione groups (Nakamoto, 1970 and Aggrawal & Narang, 1973)}. Large change is observed on the spectra of its complexes with a new $\pi \rightarrow \pi^*$ and $n \rightarrow \pi^*$ band at 35714 - 34246 and 23255 - 26456 cm^{-1} suggesting the coordination of these groups to the central metal ion. Large change is observed in the spectra of complexes with a new $n \rightarrow \pi^*$ band at 19885 - 20920 cm^{-1} , suggesting the coordination of nitrogen atom of NH group and sulfur atom of deprotonated SH group with the central metal ion (Jones, 1958).

The electronic spectrum of $[\text{Co}_2(\text{H}_4\text{ETS})\text{Cl}_2] \cdot 10\text{H}_2\text{O}$ in DMSO exhibits a well defined band at 14534 and 15923 cm^{-1} . The second band is assigned to $^4\text{A}_2(\text{F}) \rightarrow ^4\text{T}_1(\text{F})(\nu_3)$ transition characteristic for tetrahedral geometry. The band in the region 4500 - 7500 cm^{-1} cannot be observed due to restriction of our equipment. The dark green color is an additional evidence for this structure. The values of ligand field parameters (Dq , B and β) are 393 cm^{-1} , 727 cm^{-1} and 0.75 which are typical for tetrahedral

Co²⁺ complexes (Lever, 1984). The value of β indicates an appreciable degree of covalency of the Co(II) ligand bonds (El-Metwally et al., 2005). Also, the low magnetic moment value per one atom is referred to Co-S bonding in addition to strong M-M interaction. On the other hand, the spectrum of [Ni(H₅ETS)(OH)]H₂O exhibits a broad band at 15151 cm⁻¹ (ν_2) may be assignable to ¹A_{1g} → ¹A_{2g} transition and the other band at 26041 cm⁻¹ (ν_3) is due to spin-forbidden transition (Geary, 1971). Also, the diamagnetic behavior of the complex as well as the piege color are an additional evidence of the proposed structure. The spectrum of [Cu₂(H₄ETS)Cl₂] . 2H₂O complex shows a band at 20833 cm⁻¹ assignable to Cl → Cu (II) transition (Speier et al., 1996); Hathaway & Billing, 1970) and Hathaway, 1984) supporting the coordination via terminal chloro-ligand to Cu(II) atom. The band observed at 23364 cm⁻¹ is attributable to S → Cu transition (Khan et al., 1989 and Yokoi & Chikira, 1975). The d-d band 12468 cm⁻¹ appears as broad or weak shoulder in the tail of CT bands is due to ²B_{1g} → ²A_{1g} and ²B_{1g} → ²E_g transitions, respectively, in a square planar arrangement. Also, the subnormal magnetic moment value per copper atom ($\mu_{\text{eff.}} = 1.14$ B.M.) reveals the strong Cu-Cu interaction.

Table (3): Magnetic moments and electronic spectral data of H₆ETS and its Complexes.

Complex	State	μ_{eff} (B.M.)	Intraligand and d-d transition bands (cm ⁻¹)	Ligand field parameters		
				Dq	B	β
H ₆ ETS	DMSO	---	36496, 26455, 17301	----	----	--
	Nujol		-----	----	----	--
[Cu ₂ (H ₄ ETS)Cl ₂].2H ₂ O	DMSO	1.14	35714, 26455	----	----	--
	Nujol		23364, 20833, 19920, 17793, 12468	----	----	--
[Co ₂ (H ₄ ETS)Cl ₂].10H ₂ O	DMSO	2.57	34482, 26178, 16722	3935.9	727.9	0.75
	Nujol		23041, 19685, 17857, 15923, 14534			
[Ni(H ₅ ETS)(OH)].H ₂ O	DMSO	---	34246, 26041	----	----	--
	Nujol		23255, 20920, 18315, 17730, 15151			

3.5. Electron spin resonance

The room temperature solid state ESR spectrum of the binuclear $[\text{Cu}_2(\text{H}_4\text{ETS})\text{Cl}_2] \cdot 2\text{H}_2\text{O}$ complex is shown in Fig.3 and the spin Hamiltonian parameters of the complexes are calculated and summarized in **Table 4**. The spectrum exhibits an axially symmetric g-tensor parameters with $g_{\parallel} > g_{\perp} > 2.0023$ indicating that the copper site has $d_{x^2-y^2}$ ground state characteristic of square-planar, or octahedral stereochemistry (**Gregson et al., 1971**). In axial symmetry the g-values are related by the expression, $G = (g_{\parallel} - 2) / (g_{\perp} - 2) = 4$. The calculated G value for the present Cu^{2+} complex is less than 4 suggesting copper-copper interactions (**Sacconi & Ciamolini, 1964**) which is consistent with the magnetic moment value ($\mu_{\text{eff}} = 1.14$ B.M.). A forbidden magnetic dipolar transition for the complex is observed at half-field (ca. 1600 G, $g \approx 4.0$) confirming the bi-molecular nature of the complex (**Stephenson & Wilkinson, 1967**). The EPR spectrum of the complex exhibits a broad single line, nearly isotropic signal centered at $g = 2.06$ (**Fig.3**) which is attributable to dipolar broadening and enhanced spin lattice relaxation (**Speier et al., 1996**). This line broadening is probably due to insufficient spin-exchange narrowing toward the coalescence of four copper hyperfine lines to a single line. Note that, the same kind of powder EPR line shapes have also been observed for many distorted-tetragonal Cu^{2+} complexes (**Hathaway & Billing, 1970 and Hathaway, 1984**). The distortion index, $f(\alpha) = g_{\parallel} / A_{\parallel}$ of the increase of the tetrahedral distortion in the coordination sphere is the decrease of A_{\parallel} with an increase of g_{\parallel} (**Khan et al., 1989**). To quantify the degree of distortion of the Cu^{2+} complexes, the f-factor $g_{\parallel} / A_{\parallel}$ was calculated which is considered as an empirical index of tetrahedral distortion (**Yokoi & Chikira, 1975**). Its value ranges between 105 and 135 for square-planar complexes, depending on the nature of the coordinated atoms. In the presence of a distorted-tetrahedral structure, the values can be much larger (**Khan et al., 1989**). For the studied complex the factor was 157 demonstrating the existence of significant dihedral angle distortion in the xy-plane and indicating a tetrahedral distortion from square-planar geometry. The results are consistent with distorted-tetragonal geometry around the copper site.

The molecular orbital coefficients, α^2 (a measure of the covalency of the in-plane σ -bonding between a copper 3d orbital and the ligand orbitals) and β^2 (covalent in-plane π -bonding), were calculated by using the following equations (**Yokoi & Chikira, 1975; Pal & Proc, 2002**;

Wellman & Hulsbergen, 1978; Kasumov, 2001 and Raman et al., 2001):

$$\alpha^2 = (A_{\parallel}/0.036) + (g_{\parallel} - 2.0023) + 3/7(g_{\perp} - 2.0023) + 0.04$$

$$\beta^2 = (g_{\parallel} - 2.0023)E / -\lambda\alpha^2$$

Where $\lambda = -828 \text{ cm}^{-1}$ for the free copper ion and E is the electronic transition energy. The values of α^2 and β^2 for the complex indicates that the in-plane σ -bonding and in-plane π -bonding are appreciably covalent, and are consistent with very strong in-plane σ -bonding in this complex. For the Cu(II) complexes, the high values of α^2 compared to β^2 indicate that the in-plane π -bonding is less covalent than the in-plane σ -bonding. These data are well consistent with other reported values (John, 2003; Al-Hazmi et al., 2005; El-Metwally et al., 2006; Kiverlson & Lee, 1964 and El-Metwally et al., 2005).

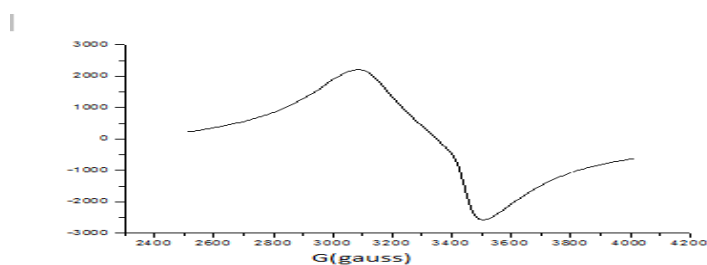


Fig.(3).ESR spectrum of $[\text{Cu}_2(\text{H}_4\text{ETS})(\text{Cl})_2] \cdot 2\text{H}_2\text{O}$

Table (4): ESR data of the some Cu II) complex at room temperature.

Complex	g_{\parallel}	g_{\perp}	$A_{\parallel} \times 10^{-4} \text{ cm}^{-1}$	G	$g_{\parallel} / A_{\parallel}$	α^2	β^2
$[\text{Cu}_2(\text{H}_4\text{ETS})\text{Cl}_2] \cdot 2\text{H}_2\text{O}$	2.24	2.08	142	3.02	157	0.66	0.69

3.6. Mass spectral studies

The mass spectrum of H_6ETS (Fig.4) shows the parental ion peak at $m/z = 497.35$ corresponding to $(\text{C}_{24}\text{H}_{28}\text{N}_6\text{S}_2\text{O}_2)$. The different fragments of the compound give the peaks with various intensities at different m/z values like at 50 (C_4H_4), 94 ($\text{C}_5\text{H}_6\text{N}_2$), 126 (C_{10}H_6), 158 ($\text{C}_7\text{H}_4\text{N}_3$), 189 ($\text{C}_8\text{H}_{10}\text{N}_5$), 178 ($\text{C}_{14}\text{H}_{10}$) (and 420.45 ($\text{C}_{20}\text{H}_{16}\text{N}_5\text{S}_2\text{O}$))

the fragmentation path of H₆ETSis given in scheme 1 (Warad et al., 2000).

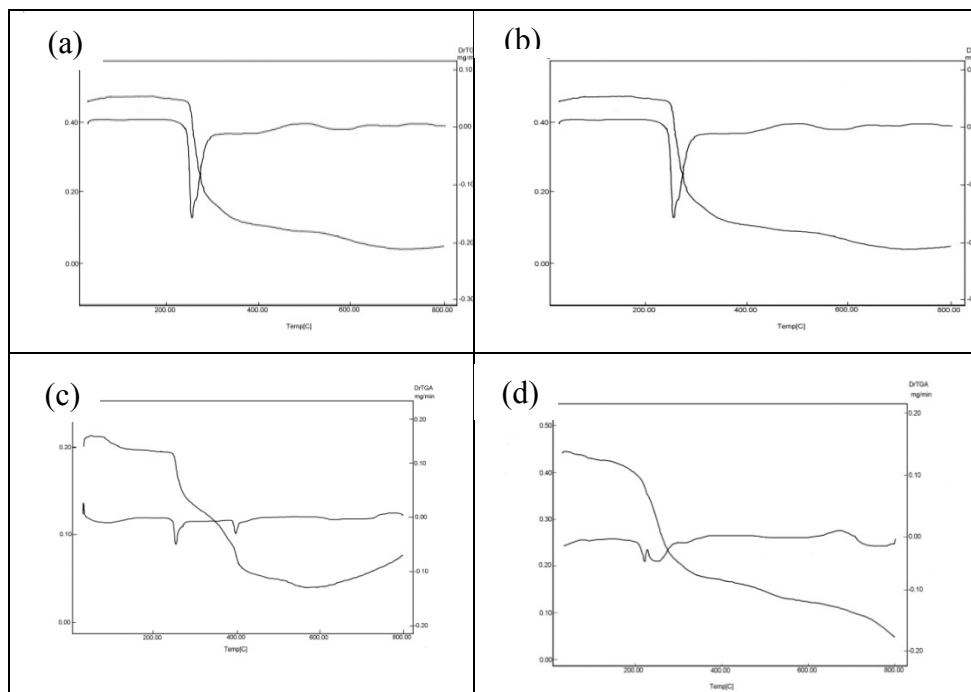
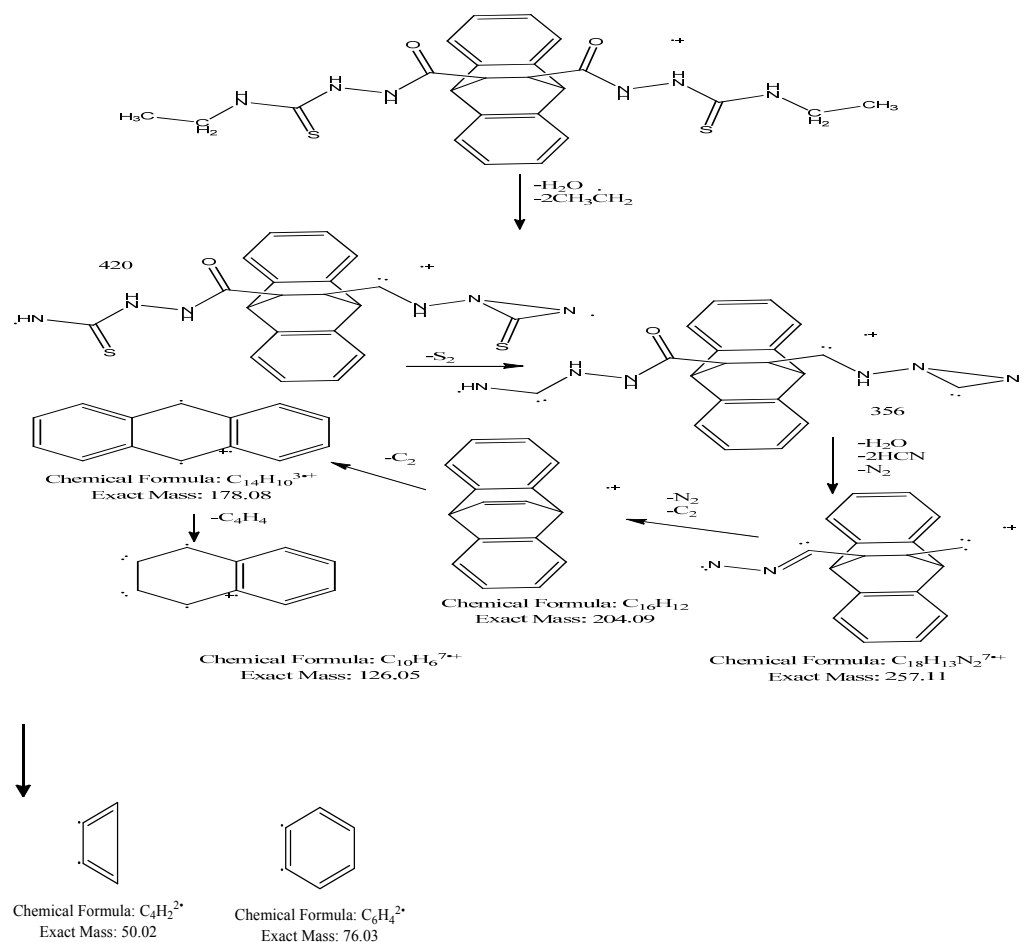


Fig. (4): Thermal analysis curves of :

- (a) H₆ETS (b) [Co₂(H₄ETS)Cl₂].10 H₂O
 (c) [Ni(H₅ETS)(OH)] and (d) [Cu₂(H₄ETS)(Cl)₂].2H₂O



Scheme 1

3.7. Thermogravimetric studies

The stages of decomposition, temperature range, decomposition product as well as the weight loss percentages of complexes are given in Table 5. One of the features in TGA data concerning the associated water and/or ethanol molecules within the complexes supports the elemental analyses. Water of crystallization was lost within the temperature range 38-114 °C. Figure 3 shows the TGA curves of the compounds under study. TG curve of $[Cu_2(H_4ETS)Cl_2] \cdot 2H_2O$ complex as a representative example displays four degradation steps. The first step at 38-107 °C with weight loss of 4.52 (Calcd. 4.94 %) is attributed to the

loss of the two lattice water molecules. The second step with weight loss of 9.34 (Calcd. 9.88 %) at 108-227°C is corresponding to the removal of HCl. The third step at 228-301 °C with weight loss of 31.72 (Calcd. 31.58%) is referring to the removal of HCl+2H₂S+CH₃CH₂NH₂ fragments. The fourth step (302-620°C) can be ascribed to elimination of 2C₆H₅+ 2 N₂ fragments with weight loss of 20.65 (Calcd. 20.00 %). The residual part is 2CuO+8C(Found 33.41, Calcd. 33.35%).

Table (5): Decomposition steps with the temperature range and weight loss for H₆ETS and its complexes.

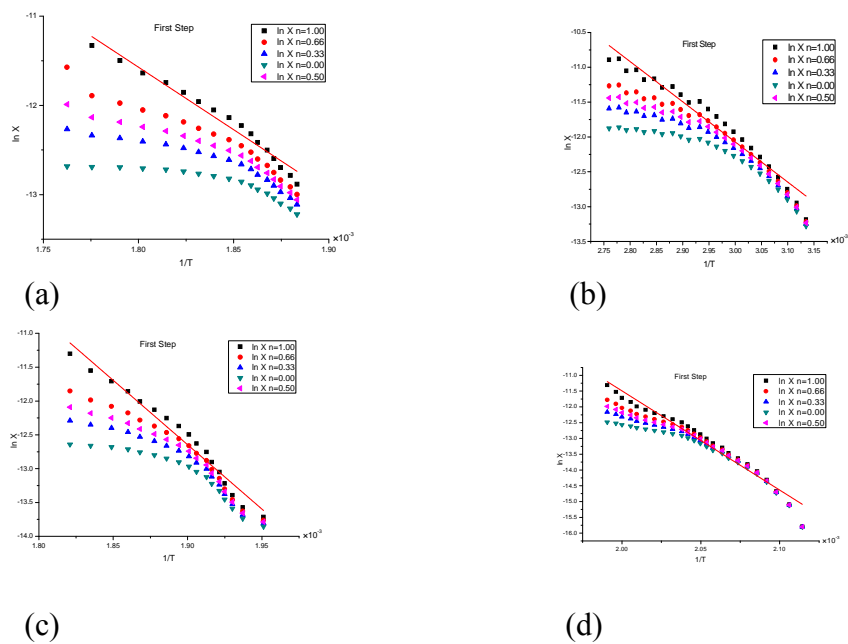
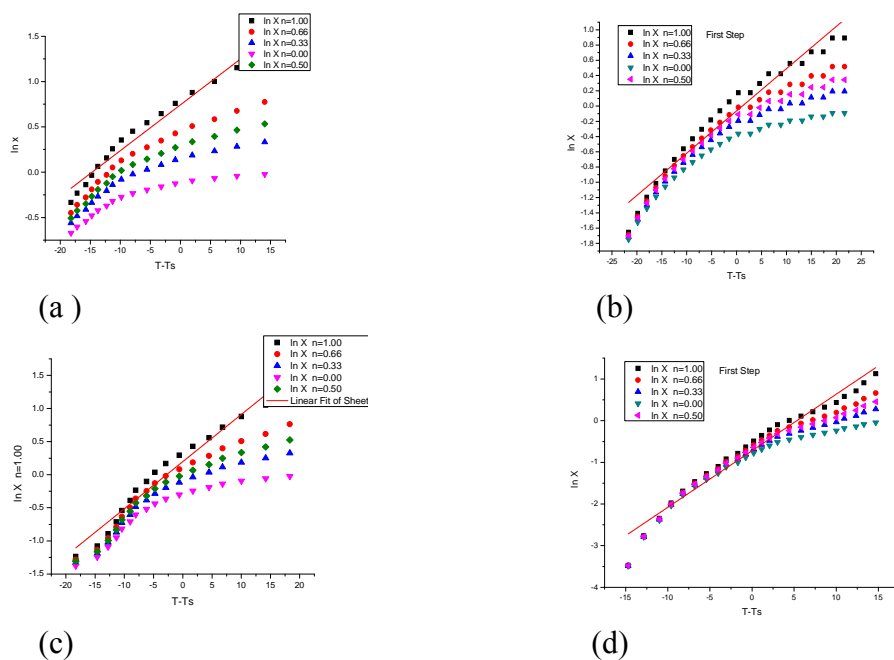


Fig 5. Coats-Redfern plots of 1ststep of (a) H_6ETS (b) $Co_2(H_4ETS)Cl_2 \cdot 10H_2O$ (c) $[Ni(H_5ETS)(OH)]H_2O$ and (d) $[Cu_2(H_4ETS)(Cl)_2] \cdot 2H_2O$



Fig(6): Horowitz-Metzger plots of 1ststep of (a) H₆ETS (b)[Co₂(H₄ETS)CL₂].10 H₂O (c)[Ni(H₅ETS) (OH)] and (d) [Cu₂(H₄ETS)(Cl)₂].2H₂O

3.8. Kinetic data

The kinetic and thermodynamic parameters of thermal degradation process using Coats-Redfern and Horowitz-Metzger models (Coats & Redfern, 1964 and Horowitz & Metzger, 1964) have been evaluated (Tables 6&7) and the data represented graphically in Figs. 5 &6. A number of pyrolysis processes can be represented as a first order reaction. The enthalpy of activation, ΔH*, entropy of activation, ΔS* and free energy of activation, ΔG* (Tables 6&7) were calculated by Eyring equation(Broido, 1969):

$$\Delta H^* = E_a - RT$$

$$\Delta S = R \ln \frac{hA}{k_B T}$$

$$\Delta G^* = \Delta H^* - T\Delta S^*$$

Table 6: Kinetic parameters evaluated by Coats-Redfern equation.

The high values of the energy of activation, E_a of the complexes reveal the high stability of such chelates due to their covalent bond character (**Mortimer, 2000**) and the positive sign of ΔG^* for the investigated complexes indicates that the free energy of the final residue is higher than that of the initial compound, and all the decomposition steps are non-spontaneous processes. Also, the values of the activation, ΔG^* increases significantly for the subsequent decomposition stages of a given complex. This is due to increasing the values of $T\Delta S^*$ significantly from one step to another which overrides the values of ΔH^* (**Frost & Pearson, 1961**). The entropy of activation, ΔS^* has negative values indicating more ordered activated complex than the reactants or the reaction is slow (**Kandil et al., 2004**).

Table (7): Kinetic parameters evaluated by Horowitz-Metzger equation.

3.9. Biological Studies

3.9.1. DNA electrophoresis

The degradation effect of 15 μ M of H₆ETS and its metal complexes on the DNA in vitro is illustrated in Fig. 7. Both the -ve control (only DNA) and +ve control (DNA in DMSO) does not exhibit any degradation effect through the incubation period. H₆ETS exhibits a weak degradation effect on the DNA. However, the Cu(II) and Co(II) complexes degrades the DNA more than H₆ETS and Ni(II) complex. The result may suggest that the Cu(II) and Co(II) complexes at 15 μ l concentrations can be used as a hopeful antitumor agent in vivo to hold back the DNA replication in the cancer cells and prevent the tumor for further growth.

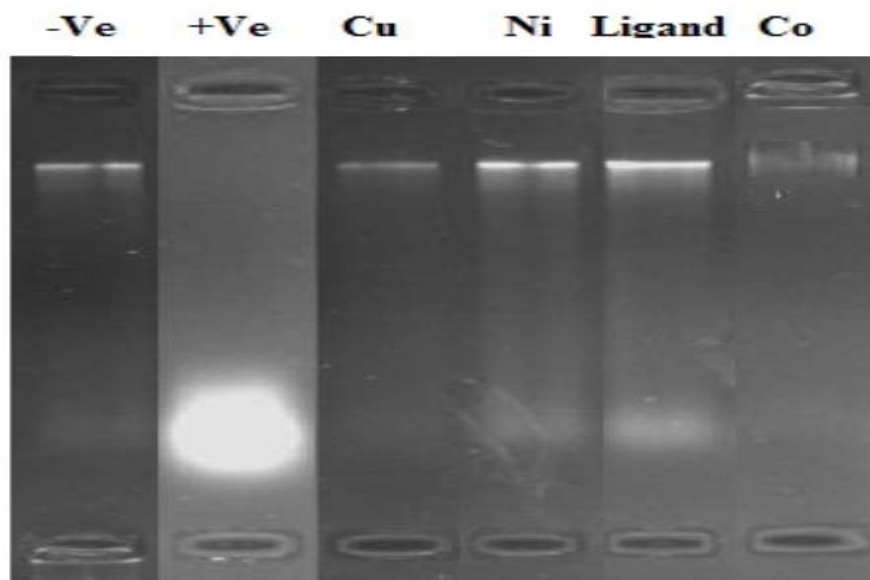
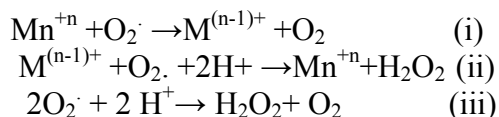


Fig. (7): Effect of 10 μ M of H₆ETS and its metal complex on the DNA *in vitro*

3.9.2. Scavenging activities of superoxide radicals

Even under optimal circumstances, reactive oxygen species (ROS), including the superoxide radical O_2^- , the hydroxyl radical ($\cdot OH$) and hydrogen peroxide (H_2O_2) produced as a byproduct of normal metabolism in different subcellular compartments (**Asada et al., 1999**). The ROS can damage DNA, proteins, membrane functions, generate lipid peroxidation and have been implicated in the pathology of a vast variety of human diseases like cancer, diabetes, hypertension and aging (**Lee et al., 2000**). To mitigate and repair damage of DNA initiated by ROS, cells have developed a complex antioxidant system. Superoxide dismutase (SOD) is the first line of defense against injury caused by ROS, catalyzing the dismutation of O_2^- to H_2O_2 , and molecular oxygen (**del Río et al., 2002**). It is important to find SOD mimics, which have the activity of SOD and at the same time, are stable. Dismutation of superoxide forms hydrogen peroxide and in the presence of transition metals, the Fenton reaction produces hydroxyl radicals from the substrate hydrogen peroxide (**Ken et al., 2005**). There are two kinds of

SOD mimics: metal-dependent and metal-independent mimics. This work focused on the metal dependent SOD mimics, their assays, chemical characters and usage. SOD or the metal complexes catalyze the dismutation of superoxide according to the following equations:



In the present study H₆ETS ligand and its metal complexes were screened for their superoxide-scavenging activity in the PMS/NADH–NBT system, and the results are represented in **Table 8**. In this system, superoxide anion derived from dissolved oxygen by PMS/NADH coupling reaction reduces NBT. The decrease of absorbance at 560 nm with antioxidant activities of the complexes indicates the consumption of superoxide anion in the reaction mixture. There is an apparent variation in the overall scavenging ability among the parent ligand and its metal complexes. The ligand had the potent activity comparable to ascorbic acid followed by Ni(II) and Co(II) complexes displaying 100 % scavenging activities of the superoxide radical. On the other hand, Cu (II) complex revealed activity lower than 50%. Superoxide is a major factor in radiation damage, inflammation and tumor promotion. Fortunately, the present study has evolved a defense system against the toxicity of O₂ •- by the ligand and its Ni(II) and Co(II) complexes.

Table(8): Effect of H₆ETS and its metal complex on superoxide radicals generated by PMS/NADH system.

compound	Δ through 5 min	% inhibition
Control	0.420	-
L- Ascorbic	0.083	80.23
H ₆ ETS (1)	0.082	80.47
Cu(II) (2)	0.303	27.85
Co(II) (3)	0.112	73.33
Ni(II) (4)	0.106	74.76

3.9.3. Scavenging activities of hydroxyl radicals

The data of the scavenging effect of H₆ETS and its metal complexes on hydroxyl radicals that generated by the oxidation of cytochrome *c* in L-ascorbic acid/CuSO₄-cytochrome *c* system are recorded in **Table 9**. Co(II) complex exhibited the highest-scavenging activity more (95.61%) followed by Cu(II)(89.91%) and Ni(II)(70.61%) complexes while H₆ETS showed scavenging activity lower than 50%.

Table (9): Effect of H₆ETS and its metal complexes on hydroxyl radicals generated by l-ascorbic acid/Cu²⁺ system.

Compound	OD ₅₅₀	% inhibition
Control	0.198	-
Thiourea	0.654	100
H ₆ ETS (1)	0.231	7.23
Cu(II) (2)	0.608	89.91
Co(II) (3)	0.634	95.61
Ni(II) (4)	0.520	70.61

3.9.4. Antibacterial activity

The zone of inhibition was measured in mm and the values of the investigated compounds are summarized in Table 10. A glance at the Table indicate that the ligand had no antibiotic activity while Cu(II) complex exhibited the highest inhibition activity against all bacterial organisms. On the other hand, Co(II) and Ni(II) complexes exhibited only a moderate activity against *Staphylococcus epidermalies* (*St.epid*). Such increased activity of the metal complexes can be explained on the basis of the Overtone concept and chelation theory (**Raman et al., 2003**). According to the overtone concept of cell permeability, on chelation, the polarity of the metal ion is reduced to a great extent due to the overlap of the ligand orbital and the partial sharing of the positive charge of the metal ion with donor groups so increases the delocalization of electrons over the whole chelate ring and enhances the lipophilicity of the complex. Consequently, enhances the penetration of the complex into the lipid membrane and blocks the metal binding sites on the enzymes of the microorganism.

Table(10):The antibacterial activity of H₆ETS and its metal complexes in terms of inhibition zone diameter (mm).

compound	E. coli	Staph. epidermalie s	Klebsiella Species	Strep. Pyogenies
Amp.	12	15	14	18
H ₆ ETS	-	-	-	-
Ni(II)	-	9	-	-
Co(II)	-	7	-	-
Cu(II)	10	23	15	10

Amp.= Ampicilline

3.9.5. Structure activity relationship (SAR) studies

1. In antibacterial and DNA degradation assay, Cu(II) and Co(II) had displayed the potent activity which may referred to the presence of the two halogens(Cl⁻) and two metal chelate rings in the molecules. On the other hand in Ni(II) complex, there is only no Cl⁻ and one chelate ring (**Raman et al., 2003**).

2. In the free radical scavenging study, four parameters, namely the steric hindrance, the extent of availability of NH groups as electron donor or hydrogen radical, the number of OH or Cl groups and LUMO (the energy of the lowest unoccupied molecular orbital of radical) were responsible for antioxidant activity. So, H₆ETS exhibited the potent scavenging activity as the steric effects of the ring system, six NH, two C=O and two C=S groups free that can donate hydrogen atoms thus contribute to increase the antioxidant activity (**Shih & Ke, 2004**). In case of Ni(II) complex, there are still five NH, one C=S and one C=O groups free. In Cu(II) complex, there are only four NH and two C=O groups free but no C=S group. So the decrease in the number of donor groups specially NH and C=S diminishes the free radical scavenging activity and vice versa.

CONCLUSION

H₆ETS forms mononuclear Ni complex with Ni²⁺ and binuclear complexes with Co²⁺ and Cu²⁺. All the measurements confirmed tetrahedral geometry for Co²⁺ and square-planar for Cu²⁺ and Ni(II) complexes. Also, the ESR spectral data of Cu²⁺ complex are in accordance with the proposed structures. The higher values of α^2 and β^2 in case of copper complex revealed appreciable covalency in the metal-ligand bonding, presumably arising out of Cu²⁺-thione/thiol coordination. The TG analysis for the investigated complexes displayed high residual part indicating high stability of the formed chelates. Moreover, H₆ETS and complexes (Co(II) & Ni(II)) were found to be much better free radical scavenger comparable to that of vitamin C. On the other hand, Cu(II) had the potent antibacterial activity against the four bacterial organisms. Co(II) and Ni(II) complexes exhibited moderate antibacterial activity only against *Staphylococcus epidermalis*.

REFERENCES

- Abou-Melha. K.S, Farukj. H, Iran.Chem.Soc.5(10) **(2008)**122-134.
- Aeschlach. R, Loliger. J, Scott. C.B, Murcia .A, Butler. J, Halliwell .B, Aruoma .I.O, Food Chem. Toxicol. 32 **(1994)** 31-36.
- Aggrawal. R.C, Narang. K.K, Inorg.Chem.Acta. 7 **(1973)** 651-657.
- Al-Hazmi .G. A. A, El-Shahawi. M. S, Gabr. I. M, El-Asmy. A. A, J. Coord. Chem. 58 **(2005)** 713-719.
- Ali. M. A, Mirza. A. H, Monsur. A, Hossain. S, Nazimuddin .M, Polyhedron. 20 **(2001)**1045-1052.
- Alliage. C, Lissi. E.A,Int.J.Chem.Kinet.30 **(1998)** 565-570.
- Alsop. L, Cowly. A. R, Dilworth .J. R, Donnely. P. S, Peach. J. M, Rider. J.T, J. Inorg.Chim. Acta.358 **(2005)** 2770-2780.
- Asada. K, Annu. Rev. Plant Phys. and Plant Mol. Bio.50 **(1999)** 601-639.
- Back .D.F, de Oliveira. G.M, Ballin. M.A, Corbellini. V.A,Inorg. Chim.Acta. 363 **(2010)** 807-817.
- Bouwman .E, Driessen .W. L, Reedjik. J, Coord. Chem. Rev. 104 **(1990)** 143-172.
- Braibanti, A. Delavalla F, Pellinghelli. M.E. Laporti, E. Inorg. Chem.7 **(1968)** 430-437
- Broido, A, J. Polymer Sci.7 **(1969)** 1761-1773.
- Bullok. J.I, Tajmir-Riahi .H.A, J.Chem.Soc.Dalton Trans. **(1978)** 34-43.
- Campbell. M. J. M, Coord. Chem. Rev. 15 **(1975)** 279-319.
- Chikate. R.C, Belapure. A.R, Padhye .S.B, West. D.X,Polyhedron.24 **(2005)** 889-899.
- Coats .A. W, Redfern. J. P, Nature.201 **(1964)** 68-69.

del Río. L.A, Corpas. F.J, Sandalio. L.M, Palma. J.M, Gómez. M , Barroso. J.B,J. Exp. Bot.53 (2002) 1255-1272.

Delley. B, Int. J. Quantum Chem. 69 (1998) 423-433.

Delley. B, J. Chem. Phys. 113 (2000) 7756-7764.

Delley. B, J. Chem. Phys. 92 (1990) 508-517.

Delley. B, Phys. Rev. B 65 (2002) 85403-85409.

El-Asmy, A.A. Shaibi, Y.M, Shedaiwa. I.M, Khattab. M.A, Synth. React Inorg. Met-Org. Chem. 20 (1990) 461-470.

El-Ayaan. U, Youssef. M.M, Al-Shihry .S, J. Mol. Struct.936 (2009) 213-219.

El-Gammal. O.A, El-Asmy .A.A, J.Coord.Chem.61(14) (2008) 2296-2306.

El-Gazzar, A.B.A. Youssef. A.M.S. Youssef. M.M. Abu-Hashem .A.A, Badria. F.A, Eur. J. Med. Chem. 44 (2009) 609-624.

El-Metwally .N.M, El-Shazly .R. M, Gabr, I.M., El-Asmy, .A.A, Spectrochim. Acta. A 61 (2005) 1113-1119.

El-Metwally. N. M, Gabr. I. M, Abou-Hussen .A. A, El-Asmy. A. A, J. Trans. Met. Chem. 31 (2006) 71-78.

El-Shazly .R.M, Al-Hazmi .G.A.A, Ghazy. S.E, El-Shahawi .M.S, El-Asmy .A.A, Spectrochim.Acta. A60 (2004) 3187-3196.

Ferrari. M. B, Capacchi. S, Pelosi .G, Reffo. G, Tarasconi. P, Albertini. R, Pinell. S, Lunghi. P, Inorg. Chim.Acta. 286 (1999) 134-141.

Frost, A.A. Pearson. R.G, "Kinetics and Mechanisms" Wiley, New York, (1961).

Geary. W.J, Coord.Chem.Rev.7 (1971) 81-122.

Co(II), Cu(II) and Ni (II) Complexes of Novel Thiosemicarbazide. 155

Gregson .A.K, Martin R.L , Mirta. S, Proc.Roy.Soc.320 **(1971)** 473-486.

Hammer. B, Hansen .L.B, Nřskov. J.K, Phys. Rev.B59 **(1999)** 7413-7421.

Hathaway, B. J., Billing. D. E, Coord. Chem. Rev.5 **(1970)**143-207.

Hathaway. B. J, Struct. Bonding (Berlin).57 **(1984)** 55-118.

Hehre. W.J, Radom. L, Schlyer. P.V.R, Pople. J.A, Ab Initio Molecular Orbital Theory, Wiley, New York, **(1986)**.

Horowitz. H, Metzger. G, Anal. Chem.35 **(1964)** 68-69.

Hyper Chem version 8.0 Hypercube, Inc., **(2002)**.

John. R. P,Spectrochim. Acta. A59 **(2003)** 1349-1358.

Jones. L.H, Spectrochim.Acta.10 **(1958)** 395-403.

Kandil. S. S, El-Hefnawy. G. B, Baker. E. A,Thermochim. Acta.414 **(2004)** 105-278.

Kasumov. V. T, Spectrochim. Acta. A57 **(2001)** 1649-1662.

Ken. C.F, Lee. C.C, Duan .K.J, Lin. C.T, Protein Exp. Purif.40 **(2005)** 42-50.

Kessi. A, Delley. B, Int. J. Quantum Chem. 68 **(1998)** 135-144.

Khan. O, Mallah. T, Gouteron. J, Jeanin. S, Jeanin. Y, J. Chem. Soc. Dalton Trans. **(1989)** 1117-1126.

Kiverlson .D, Lee. S.K, J.Chem.Phys.41 **(1964)** 1896-1946.

Lee .Y.M, Kim. H, Hong. E.K, Kang. B.H, Kim. S.J,J. Ethnopharma.73 **(2000)** 429-439.

Lever, A.B.P. "Inorganic Electronic Spectroscopy", 2nd Edn., Elsevier, Amesterdam, **(1984)**.

Lever. A.B.P, "Inorganic Electronic Spectroscopy ", 3rd Edn., 307, 343, Elsevier, Amsterdam, **(1968)**.

Li. Z, Zhang. Y, Wang. Y, Phosphorous.Sulphur. Silicon Relat. Elem.178 **(2003)** 293-297.

Lissi. E, Modak .B, Torres. R, Escobar. J, Urza .A, Free Radical Res.30 **(1999)** 471-477.

Matveev. A, Staufer. M, Mayer. M, Rösch. N, Int. J. Quantum Chem.75 **(1999)** 863-873.

McMillian. D. R, Engeseth. H. R, Karlin. K. D, J. Zubieta (Eds.) Biological and Inorganic Copper Chemistry, Adenine Press, Guilderland,NY, **(1986)**.

Mortimer. R. G,"Physical Chemistry" A. Harcourt and Science Technology Company, Academic Press, San Diego, **(2000)**.

Mostafa. M.M,Spectrochim.Acta. A 66 **(2007)** 480-486

Nakamoto.K, "Infrared Spectra of Inorganic and Coordination compounds", 3rd Edn., Wiley, New York, **(1970)**.

Nomiya .K, Sekino. K, Ishikawa.M, Honda.A, Yokano. M, Onodera. K, J.Inorg.Biochem. 98 **(2004)** 801-807.

Pal. S, Proc. Indian Acad. Sci. 114 **(2002)** 417-430.

Petering .H. G, Burskirk. H. H, Crim .J. A, Cancer Res. 27**(1967)** 1115-1121.

Raman .N, Muthuraj. V, Ravichandran. S, Kulandaisamy. A, Proc.Ind. Acad.Sci. **(2003)** 115-161.

Raman. N, Pitchaikani Raja .Y, Kulandaisamy. A, Proc. Ind. Acad.Sci. 113 **(2001)** 183-189.

Rao. C.N.R, Venkataraghavan. R, Spectrochim.Acta .A18 **(1962)** 541-547.

Co(II), Cu(II) and Ni (II) Complexes of Novel Thiosemicarbazide. 157

Rapheal. P.F, Manoj. E, Prathapachandar Kurup. M.R, Polyhedron.26 (2007) 818-828.

Sacconi. L, Ciamolini .M, J.Chem.Soc. (1964) 276-280.

Shih .M. H, Ke. F. Y, Bioorg. Med. Chem. 12 (2004) 4633-3643.

Speier. G, Csihony. J, Whalen .A. M, Pie-Pont. C. G, Inorg. Chem. 35 (1996) 3519-3524.

Stephenson. T. A, Wilkinson .G, J. Inorg. Nucl. Chem. 29 (1967) 2122-2123.

Syamal. A , Kale. K.S, Indian J.Chem. A 16 (1998) 46-51.

Wada. K, Fujibayahsia .Y, Yokoyama .A, Arch. Biochem. Biophys. 310 (1994)1.

Warad. D.U, C.D.Statish, V.H.Kulkarni, C.S.Bajgur, Ind J.Chem.A 39 (2000) 415-420.

Wellman. J. A, Hulsbergen. F. B, J. Inorg. Nucl.Chem.40 (1978) 143-146.

West. D. X, Liberta .A. B, Padhye .S. B, Chikate. R. C, Sonawane. A. S, Kumbhar .P. B, Yerande. R. G, Coord. Chem. Rev. 123 (1993) 49-71.

West. D. X, Padhye. S. B, Sonawane. P. B, Struct. Bond. 76 (1991)1-50.

West. D.X, Swearingen. J.K, Valdés Martinez. J, Hernández-Ortega. S, El-Sawaf.A.K, Van Meurs.F, Castiñeiras.A, Garcia. I, Bermejo.E, Polyhedron.18 (1999) 2919-2929.

Yokoi. H, Chikira. M, J. Am. Chem. Soc.97 (1975) 3975-3978.

تحضير وتمييز النشاط البيولوجي لمعقدات ثنائية السالبيية لكل من الكوبلت والنحاس بينما يكون أحادي السالبيية في معقد النيكل وهذه المعقدات تكون من ضمن مترابطات الثيوسيميكرابازيدات الضخمة ومتعددة المخلبية.

د/علا أحمد الجمال .أ.د/أحمد فوزي العاصمي .أبتسام محمد عبدالقادر

تم دراسة السلوك المخاببي للثيوسيميكرابازيد متعدد الترابط (-2,2', 9,10-dihydro-9,10-ethanoanthracene-11,12-((9S,10S,11R,12R) (H₆ETS)(dicarbonyl)bis(N-ethylhydrazine-1-carbothioamide) تجاه بعض ايونات العناصر الانتقالية (Co²⁺, Ni²⁺ and Cu²⁺) وتم استنتاج شكل المترابطات بالقياسات المختلفة وأثبتت النتائج أن المرتبط يعمل ك رباعي الاعطاء أحادي السالبيية (NNSS) في العقد Cu²⁺ أو NOS سداسي المخلبي في معقدات الكوبلت النيكل الثنائية .

من خلال دراسة الطيف الالكتروني والقياسات المغناطيسية تم استنتاج أن معقدات النيكل والنحاس الثنائية تكون في شكل مربع المستوي من ناحية الشكل الفراغي أما الكوبلت يكون هرم رباعي. من خلال دراسة الرنين النووي المغناطيسي لمعقد النحاس وجد أنه يعمل ك axial spin-) (Hamiltonian) وبالتالي تعطي أربعة خطوط في (pattern with nitrogen super-hyperfine couplings originating) المتمثل في (imine hydrazinic) في درة النيتروجين.

المعقدات الموجودة في المستوى لها شكل فراغي يسمى (pseudo-square planar) حيث يحدث تشوه في الشكل الفراغي أي يتحول الى شكل الهرم الرباعي . والالكترون غير المزدوج الموجود في (d_{x2-y2} ground state) . وطول الرابطة والزوايا بين الروابط ثم حسابها أيضا .

الدراسات الحرارية والمعاملات الحركية ثم التعرف عليها من خلال طريقتي (Coats-Redfern and Horowitz-Metzger) وايضاً تم دراسة النشاط البيولوجي للمركبات وهي:-

- مضادات للبكتريا حيث تم استخدام (*St. epid*); (*Staphylococcus epidermalies*)
- (*Streptococcus pyagenies* (*Strp.py.*) التي تعمل ك Gram +ve, وكذلك (*Eserchia*)
- (*klebsiella Spp*(*kleb.spp.*) ; (*Coli*(*E.coli*) التي تعمل ك Gram -Ve حيث أستنتج أن المركبات تعمل على تثبيط البكتريا.
- (DNA) أي تكسير الحامض النووي الاميني.
- تأثير الشق الحر للهيدروكسيل.
- تأثير (superoxide-scavenging).